

Investigations of the Local Supercluster Velocity Field

II. A study using Tolman-Bondi solution and galaxies with accurate distances from the Cepheid PL -relation

Ekholm, T.^{1,2}, Lanoix, P.¹, Teerikorpi, P.², Paturel, G.¹, and Fouqué, P.³

¹ CRAL - Observatoire de Lyon, F69561 Saint Genis Laval CEDEX, France

² Tuorla Observatory, FIN-21500 Piikkiö, Finland

³ ESO, Santiago, Chile

received, accepted

Abstract. A sample of 32 galaxies with accurate distance moduli from the Cepheid PL -relation (Lanoix 1999) has been used to study the dynamical behaviour of the Local (Virgo) supercluster. We used analytical Tolman-Bondi (TB) solutions for a spherically symmetric density excess embedded in the Einstein-deSitter universe ($q_0 = 0.5$). Using 12 galaxies within $\Theta = 30^\circ$ from the centre we found a mass estimate of $1.62M_{\text{virial}}$ for the Virgo cluster. This agrees with the finding of Teerikorpi et al. (1992) that TB-estimate may be larger than virial mass estimate from Tully & Shaya (1984). Our conclusions do not critically depend on our primary choice of the global $H_0 = 57 \text{ km s}^{-1} \text{ Mpc}^{-1}$ established from SNe Ia (Lanoix 1999). The remaining galaxies outside Virgo region do not disagree with this value. Finally, we also found a TB-solution with the H_0 and q_0 cited yielding exactly one virial mass for the Virgo cluster.

Key words: Cosmology: theory – distance scale – Galaxies: distances and redshifts – Galaxies: general – Galaxies: kinematics and dynamics – Local Group

1. Introduction

When studying the dynamical properties of a structure like the Local (Virgo) supercluster (LSC) one obviously cannot use the standard solutions to the Friedman-Robertson-Walker (FRW) world model which are valid in a homogeneous environment only. General Relativity does, however, provide means for this kind of a problem, namely the so-called Tolman-Bondi (TB) model. While no longer requiring strict homogeneity, spherical symmetry is a necessary requisite. In the present paper we address the question how well the velocity field in the LSC follows the TB-prediction, i.e. how well it meets the requirement of spherical symmetry.

Previous studies (Tully & Shaya 1984; Teerikorpi et al. 1992 - hereafter Paper I) provided evidence for the expected velocity field if the mass of the Virgo cluster itself is roughly

equal to its virial mass. However, the Tully-Fisher distances used caused significant scatter. Now we possess a high-quality sample of galaxies with accurate distances from Cepheids.

Tolman (1934) found the general solution to the Einstein's field equations for a spherically symmetric pressure-free dust universe in terms of the comoving coordinates. The metric can be expressed as:

$$ds(r, \tau)^2 = d\tau^2 - \frac{R'(r, \tau)^2}{1 + f(r)} dr^2 - R(r, \tau)^2 d\Omega^2, \quad (1)$$

where $d\Omega^2 = d\theta^2 + \sin^2 \theta d\phi^2$ and $f(r)$ is some unknown function of the comoving radius r . R corresponds to the usual concept of distance. Integration of the equation of motion yields:

$$\dot{R}^2 = \frac{F(r)}{R} + f(r). \quad (2)$$

\dot{R} refers to $\partial R / \partial \tau$ and R' to $\partial R / \partial r$. $F(r)$ is another arbitrary function of r .

Bondi (1947) interpreted Eq. 2 as the total energy equation: $f(r)$ is proportional to the total energy of the hypersurface of radius r and $F(r)$ is proportional to the mass inside r . In this interpretation it is clear that one must require $F(r) > 0$. Eq. 2 integrates into three distinctive solutions. Two of them are expressed in terms of a parameter η , the development angle of the mass shell in consideration:

$$\begin{aligned} R &= \frac{F}{2f} (\cosh \eta - 1) \\ \tau - \tau_0(r) &= \frac{F}{2f^{3/2}} (\sinh \eta - \eta), \end{aligned} \quad (3)$$

for positive energy function $f(r) > 0$,

$$\begin{aligned} R &= \frac{F}{-2f} (1 - \cos \eta) \\ \tau - \tau_0(r) &= \frac{F}{2(-f^{3/2})} (\eta - \sin \eta), \end{aligned} \quad (4)$$

for negative energy function $f(r) < 0$. The third solution is for $f(r) = 0$:

$$R = \left(\frac{9F}{4} \right)^{1/3} [\tau - \tau_0(r)]^{2/3}. \quad (5)$$

It is important to note that the solution has *three* undefined functions: $f(r)$, $F(r)$ and $\tau_0(r)$. One of these can be fixed by defining some arbitrary transformation of the comoving coordinate r . In our application we set $\tau_0(r) \equiv 0$ and interpret τ as time elapsed since the Big Bang, i.e. we equal τ with the age of the Universe T_0 .

To find a TB-prediction for the observed velocity, we use the formulation of Paper I, based on the solutions given by Olsson & Silk (1979). In this approach the development angle η needed for the velocity is solved with the help of a function:

$$A(R, T_0) = \frac{\sqrt{GM(R)T_0}}{R^{3/2}}, \quad (6)$$

where R is the distance of spherical mass shell from the origin of the TB-metric, $M(R)$ is the mass contained within the shell and G is the gravitational constant. η is solved either from Eq. 7 or Eq. 8 of Paper I depending on value $A(R, T_0)$. Ekholm (1996; hereafter E96) calculated in his Appendix B the exact value of A dividing the family of solutions into open, hyperbolic solutions ($f(r) > 0$) and closed, elliptic solutions ($f(r) < 0$): $A = \sqrt{2}/3 \approx 0.47$.

2. Details of the model used

In Paper I, Ekholm & Teerikorpi (1994; hereafter ET94) and E96 one chose as a starting point a “known” mass $M(R)$ for each R inferred from some density distribution given as a sum of an excess density and the uniform cosmological background. We assume:

$$\rho(R) = \frac{3H_0^2 q_0}{4\pi G} (1 + kR^{-\alpha}). \quad (7)$$

H_0 is the Hubble constant, q_0 is the deceleration parameter. k and α define the details of the density model and will be explained shortly.

E96 further developed this formalism by defining a “local Hubble constant” $H_0^* = V_{\text{cosm}}(d=1)$, where d is calculated from Eq. 14. By setting $d = 1$ we can fix the mass excess k' independently of the density gradient α . In this manner the quantity A can be expressed in terms of d and q_0 (Eq. 7 in E96):

$$A(d, q_0) = C(q_0) \sqrt{q_0(1 + k'd^{-\alpha})}. \quad (8)$$

The factor $C(q_0)$ depends on the cosmological FRW world model chosen (cf. Eqs. 8-10 in E96). The mass contained by a shell of radius d is (Eq. 4 in E96):

$$M(d) = \frac{H_0^2}{G} q_0 R_{\text{Virgo}}^3 d^3 (1 + k'd^{-\alpha}). \quad (9)$$

k' (k normalized to the Virgo distance) provides the mass excess within a sphere of radius $d = 1$ and can be fixed from our knowledge of the observed velocity of the centre of the mass structure and of the infall velocity of the Local Group (LG) as follows. Let $V_{\text{Virgo}}^{\text{obs}}$ be the observed velocity of Virgo and $V_{\text{LG}}^{\text{in}}$ the infall velocity of the LG. The predicted velocity of a galaxy

with respect to the centre of the structure in consideration was given by E96 (his Eq. 11):

$$v(d) = \frac{\gamma d V_{\text{Virgo}}^{\text{obs}} \phi(\eta_0)}{C(q_0)} \quad (10)$$

with

$$\gamma = (V_{\text{Virgo}}^{\text{obs}} + V_{\text{LG}}^{\text{in}}) / V_{\text{Virgo}}^{\text{obs}}. \quad (11)$$

$\phi(\eta_0)$ is the angular part of Eqs. 15 and 16 given by ET94, where η_0 is the development angle corresponding to the given value of A . Hence for each $V_{\text{LG}}^{\text{in}}$ one may fix k' by requiring:

$$v(1) = V_{\text{Virgo}}^{\text{obs}}. \quad (12)$$

One clear advantage of this formulation is – being perhaps otherwise idealistic – that the value of k' depends only on the two velocities given above for a fixed FRW world model (H_0, q_0). Thus α will alter only the distribution of dynamical matter (the larger the α the more concentrated the structure).

Finally, we need the predicted counterpart of the observed velocity of a galaxy. In the present application it is solved from:

$$V_{\text{pred}}(d_{\text{gal}}) = V_{\text{Virgo}}^{\text{obs}} \cos \Theta \pm v(d) \sqrt{1 - \sin^2 \Theta / d^2}, \quad (13)$$

where $d_{\text{gal}} = R_{\text{gal}} / R_{\text{Virgo}}$ is the relative distance of a galaxy from the LG, Θ is the corresponding angular distance and d , the distance to the galaxy measured from the centre of the structure, is evaluated from:

$$d = \sqrt{1 + d_{\text{gal}}^2 - 2d_{\text{gal}} \cos \Theta}. \quad (14)$$

The (–) -sign is valid for points closer than the tangential point $d_{\text{gal}} < \cos \Theta$ and (+) -sign for $d_{\text{gal}} \geq \cos \Theta$.

3. The sample

Eq. 14 reveals one significant difficulty in an analysis of this kind. In order to find the relative distances d_{gal} one needs good estimates for the distances to the galaxies R_{gal} . Such are difficult to obtain. Distances inferred from photometric data via, say, the Tully-Fisher relation are hampered by large scatter and as a result, by the Malmquist bias which is difficult to correct for. Distances inferred from velocities using the Hubble law are obviously quite unsuitable.

The HIPPARCOS satellite has provided a sample of galactic Cepheids from which Lanoix et al. (1999a) obtained a new calibration of the PL -relation in both V and I band. Lanoix (1999) extracted a sample of 32 galaxies from the Extragalactic Cepheid Database (Lanoix et al. 1999b) and, by taking into account the incompleteness bias in the extragalactic PL -relation (Lanoix et al. 1999c), he inferred the distance moduli for these galaxies with 23 based on HST measurements and the rest on groundbased measurements. It is also important to note that the sample is very homogeneous and the method for calculating the distance modulus is quite accurate. The photometric distances found in this way are far more accurate and of better quality

than those derived using Tully-Fisher relation, a fact compensating the smallness of our sample.

We intend to use these galaxies together with the TB-model described in the previous two sections to study the gross features of the dynamical structure of the LSC. Because we need only the observed velocities, V_{obs} and the Cepheid distance moduli μ , we can avoid the usual difficulties and caveats of other photometric distance determinations. The velocities were extracted from the Lyon-Meudon Extragalactic Database LEDA. By observed velocity we refer to the mean heliocentric velocity corrected to the LG centroid according to Yahil et al. (1977).

We need, however, some additional information: $V_{\text{Virgo}}^{\text{obs}}$, $V_{\text{LG}}^{\text{in}}$ and R_{Virgo} . For the observed velocity of the centre of the LSC the value preferred by Paper I is $V_{\text{Virgo}}^{\text{obs}} = 980.0 \text{ km s}^{-1}$. For the infall velocity of the LG into the centre we choose $V_{\text{LG}}^{\text{in}} = 220 \text{ km s}^{-1}$ (Tammann & Sandage 1985). It is worth noting that though this value has fluctuated, this relatively old value is still quite compatible with recent re-evaluations (cf. Federspiel et al. 1998). Furthermore, the fluctuations have not been very significant. We also need an estimate for the distance of the centre of the LSC, R_{Virgo} . One possibility is to establish the Hubble constant H_0 from some independent method. Lanoix (1999) found using SNe Ia's:¹

$$H_0 = 57 \pm 3 \text{ km s}^{-1} \text{ Mpc}^{-1}. \quad (15)$$

This *global* value of H_0 is in good agreement with our more local results using both the direct and inverse Tully-Fisher relations (Theureau et al. 1997; Ekholm et al. 1999). H_0 and the given velocities yield $R_{\text{Virgo}} = 21.0 \text{ Mpc}$, which is in good agreement with $R_{\text{Virgo}} = 20.7 \text{ Mpc}$ found by Federspiel et al. (1998). Note also that Federspiel et al. (1998) found the same value for H_0 from relative cluster distances to Virgo. Finally, one should recognize that our distance estimate is valid only if Virgo is at rest with respect to the FRW-frame. If not, the cosmological velocity of Virgo is something more complicated than simply the sum of $V_{\text{LG}}^{\text{in}}$ and $V_{\text{Virgo}}^{\text{obs}}$.

4. Results in the direction of Virgo ($\Theta < 30^\circ$)

We restrict ourselves to the Einstein-deSitter universe by assigning $q_0 = 0.5$. As regards Eq. 8 we now possess the distance d for each galaxy as well as the value $k' = 0.606$ from Eq. 12. We also have γ from Eq. 11. We need to estimate the best value for α . We devised a simple statistical test by finding which value or values of α minimize the average $|V_{\text{obs}} - V_{\text{pred}}|$ of sample galaxies in the Virgo direction. We found minimum values around $\alpha = 2.7 - 3.0$. We adopt $\alpha = 2.85$. The resulting systemic velocity² vs. distance diagram is shown in Fig 1. The

¹ H_0 derived is not completely independent because both the SNe and the extragalactic PL -relation are calibrated with same Cepheids.

² Systemic velocity is a combination of the cosmological velocity and the velocity induced by Virgo. This is in our case the observed velocity defined in Sect. 4. It could contain also other components, but we assume that the Virgo infall dominates.

Name	Θ	V_{obs}	d_{21}	$V_{\text{pred, 1}}$	$d_{20.7}$	$V_{\text{pred, 2}}$
IC 4182	26.4	337.0	0.24	345.0	0.24	335.0
NGC 3351	26.2	640.0	0.46	666.0	0.47	545.0
NGC 3368	25.5	761.0	0.52	753.0	0.53	728.0
NGC 3627	17.3	596.0	0.42	698.0	0.43	680.0
NGC 4321	4.0	1475.0	0.71	1611.0	0.72	1593.0
NGC 4414	18.9	692.0	0.80	1098.0	0.81	1040.0
NGC 4496A	8.4	1574.0	0.72	1482.0	0.73	1453.0
NGC 4535	4.3	1821.0	0.72	1642.0	0.73	1623.0
NGC 4536	10.2	1641.0	0.65	1261.0	0.66	1235.0
NGC 4548	2.4	379.0	0.73	1710.0	0.74	1695.0
NGC 4639	3.0	888.0	1.14	-409.0	1.15	-351.0
NGC 4725	13.9	1160.0	0.58	1025.0	0.59	1001.0

Table 1. Parameters for the 12 galaxies within $\Theta < 30^\circ$ from the adopted centre of the LSC. Column 1: Name, Column 2: Angular distance Θ , Column 3: Observed velocity V_{obs} , Column 4: Relative distance with $R_{\text{Virgo}} = 21 \text{ Mpc}$, Column 5: Predicted velocity from Model 1, Column 6: Relative distance with $R_{\text{Virgo}} = 20.7 \text{ Mpc}$, and Column 7: Predicted velocity from Model 2.

observed velocities are labelled with circles and the predicted values with crosses. The straight line is what one expects from Hubble law with our choice of H_0 and the curve is the theoretical TB-solution for $\Theta = 7^\circ$ (most of the galaxies have small angular distances)³. The relative distances and predicted velocities are also tabulated in Table 1 at columns 4 and 5 for this Model 1. The galaxies follow the overall TB-pattern, with velocities steeply increasing when the Virgo center is approached. Exceptions are NGC 4639 lying at 1.14 and NGC 4548 at 0.73.

NGC 4639 has a positive velocity when – according to the model – it should be falling into Virgo from the backside. Can we explain this strange behaviour? We note it is at a small angular distance from Virgo ($\Theta = 3.0^\circ$). Perhaps NGC 4639 has fallen through the centre and still has some of its frontside infall velocity left. There are, however, no reports of significant hydrogen deficiency which one would expect if the galaxy actually had travelled through the centre. Maybe this galaxy is a genuine member of the Virgo cluster thus having a rather large dispersion in velocity. In fact, Federspiel et al. (1998) include it to their “fiducial sample” of Virgo cluster galaxies belonging to the subgroup “big A” around M87. As a matter of fact our chosen centre ($l = 284^\circ$, $b = 74.5^\circ$) lies close to the massive pair M86/87.

NGC 4548 is also close to Virgo and has a small angular distance ($\Theta = 2.4^\circ$). Now, however the situation is reversed. This galaxy should be falling into Virgo with a high positive velocity but has a small velocity. Paper I classifies this galaxy belonging to a region interpreted as a component expanding from Virgo (cf. Fig. 8 (Region B) and Table 1c in Paper I).

³ This curve is simply to guide the eye. The actual comparison is made between each observed and predicted point.

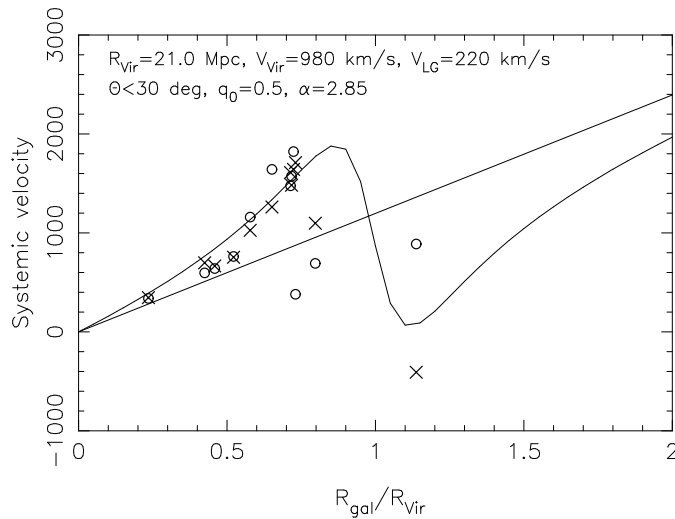


Fig. 1. The systemic velocity vs. distance for galaxies listed in Table 1 for the Model 1. Circles refer to the observed velocities and crosses to the TB-predictions. The straight line is the Hubble law for $H_0 = 57 \text{ km s}^{-1} \text{ Mpc}^{-1}$ and the curve is the theoretical TB-pattern for $\Theta = 7^\circ$. Note that the most discrepant galaxies (NGC 4639 and NGC 4548) are actually closest to the Virgo centre in the sky.

Finally, because both galaxies are close to Virgo at small angular distances even a slight error in distance determination could result in a considerable error in velocities. Hence both galaxies might follow the TB-curve but error in distance has distorted the figure.

We also tested the exact values given by Federspiel et al. (1998) with $\alpha = 2.85$. Now $V_{\text{Virgo}}^{\text{obs}} = 920 \text{ km s}^{-1}$ and $R_{\text{Virgo}} = 20.7 \text{ Mpc}$ yield with the same infall velocity $H_0 = 55 \text{ km s}^{-1} \text{ Mpc}^{-1}$. We found $k' = 0.641$. The behaviour of the systemic velocity as a function of distance is quite similar to Fig. 1. This solution is named as Model 2 and given in columns 6 and 7 in Table 1. Due to the paucity of the sample it is not possible to decide between these models.

Though we have only a few points, it is quite remarkable how well the dynamical behaviour of galaxies in the direction of Virgo is demonstrated by a simple model. That the galaxies follow so well a spherically symmetric model despite the observed clumpiness of the Virgo region is promising. Fig. 1 clearly lends credence to a presumption that the gravitating matter is distributed more symmetrically than the luminous matter. We have given an affirmative answer to the question asked in the introduction.

5. Results outside Virgo ($\Theta > 30^\circ$)

5.1. On the chosen Hubble constant

In Paper I the value of the Hubble constant was taken to be $H_0 = 70 \text{ km s}^{-1} \text{ Mpc}^{-1}$, consistent with the Tully-Fisher calibration adopted at the time and with the used Virgo distances (16.5 and 18.4 Mpc giving different infall velocities of LG). In

Name	Θ	V_{obs}	R_{Mpc}
IC 1613	163.2	-62.0	0.69
LMC	107.4	82.0	0.05
NGC 1365	132.7	1563.0	18.20
NGC 2090	106.0	754.0	11.48
NGC 224	126.3	-13.0	0.87
NGC 2541	63.8	645.0	11.59
NGC 300	154.1	125.0	2.17
NGC 3031	61.8	124.0	3.37
NGC 3109	52.7	130.0	1.02
NGC 3621	48.4	436.0	6.61
NGC 3198	43.3	704.0	13.68
NGC 4603	53.4	2300.0	32.51
NGC 5253	47.0	155.0	3.16
NGC 5457	45.7	361.0	6.92
NGC 598	134.4	68.0	0.79
NGC 6822	110.7	8.0	0.45
NGC 7331	125.9	1115.0	14.39
NGC 925	126.4	782.0	8.87
SEXA	38.8	118.0	1.45
SEXB	37.9	139.0	1.39

Table 2. Parameters for the 20 galaxies with $\Theta > 30^\circ$ from the adopted centre of the LSC. Column 1: Name, Column 2: Angular distance Θ , Column 3: Observed velocity V_{obs} , and Column 4: Distance in Mpc.

the present paper we have *fixed* H_0 from more global considerations as well as $V_{\text{LG}}^{\text{in}}$ corresponding to $R_{\text{Virgo}} = 21 \text{ Mpc}$. As discussed by ET94 once the velocity of the LG is fixed the predicted velocities no longer depend on the value of H_0 . It is still interesting to see whether the sample galaxies locally agree with $H_0 = 57 \text{ km s}^{-1} \text{ Mpc}^{-1}$. This is done in Fig. 2, where we have plotted the observed systemic velocities (open circles) outside the Virgo region ($\Theta > 30^\circ$) as a function of the absolute distance in Mpc. The data are given in Table 2. The galaxies follow quite well the quiescent flow. In particular, the closest-by galaxies ($R_{\text{gal}} < 4 \text{ Mpc}$) follow the linear prediction with surprising accuracy. Note also that galaxies listed in Table 1 (galaxies partaking in the Virgo infall) would predict $H_0 = 76 \pm 9 \text{ km s}^{-1} \text{ Mpc}^{-1}$. This too high a value clearly underlines the need for correct and adequate kinematical model in Virgo region.

However, two of the galaxies are clearly discrepant (NGC 1365 and NGC 4603) and two (NGC 925 and NGC 7331) disagree. First of all, NGC 4603 is a distant galaxy and the distance determination may be biased by the Cepheid incompleteness effect (Lanoix et al. 1999c). It also does not have a good PL -relation in V , which means that one should assign a very low weight for it. On the other hand, its velocity differs from the quiescent Hubble flow only by 375 km s^{-1} which actually is not very much considering the distance. It belongs to the Virgo Southern extension and its velocity could be influenced by the Hydra-Centaurus complex. NGC 1365 is a member of Fornax, NGC 925 belongs to the NGC 1023 group and NGC 7331 belongs to a small group near the Local Void. Under these

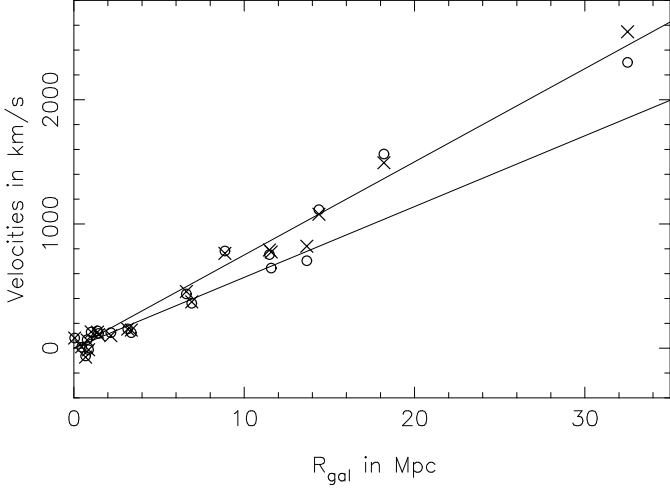


Fig. 2. The observed systemic velocity (open circles) vs. absolute distance for galaxies outside the Virgo region. The straight lines are the predictions for $H_0 = 57 \text{ km s}^{-1} \text{ Mpc}^{-1}$ from SNe Ia and for $H_0 = 75 \text{ km s}^{-1} \text{ Mpc}^{-1}$. Corrected velocities are also plotted as crosses. Note that NGC 4603 has a very bad PL relation in V and hence one should assign a low weight to it.

conditions it is not surprising that these galaxies show deviations from the Hubble law, except that they all show a tendency to have larger velocity than predicted by the Hubble law.

As can be seen from Fig. 2, these galaxies suggest a much shorter distance to Virgo (for them $H_0 = 75 \text{ km}^{-1} \text{ Mpc}^{-1}$ corresponding to $R_{\text{Virgo}} = 16 \text{ Mpc}$ would be more suitable choice for the Hubble constant). This means that without further analysis the data outside the 30° cone do not allow us to exclude a shorter distance to Virgo. We examine the effect of a short distance to Virgo on the galaxies within the 30° cone in an appendix to this paper.

Finally, we have used so far systemic velocities, i.e. velocities not corrected for the virgocentric motions. We tested how a simple correction would affect Fig. 2. The corrected velocities shown as crosses in Fig. 2 were calculated as

$$V_{\text{corr}} = V_{\text{obs}} + [v(d)_{\text{H}} - v(d)] \sqrt{1 - \sin^2 \Theta / d^2} + V_{\text{LG}}^{\text{in}} \cos \Theta, \quad (16)$$

where $v(d)$ is solved from Eq. 10 using parameters for our Model 1 and the Hubble velocity at the distance d measured from the centre of LSC is $v(d)_{\text{H}} = V_{\text{cosm}}(1) \times d$. This correction does not resolve the problem.

5.2. The nearest-by galaxies ($R_{\text{gal}} < 4 \text{ Mpc}$)

We noticed in the previous subsection that nearest-by galaxies appear to follow the Hubble law quite well. In this subsection we take a closer look at these galaxies. To begin with we note that the mean heliocentric velocities V_{\odot} (shown as filled circles in Fig. 3) have a rather large scatter but *on the mean* they agree with our primary choice of H_0 . It is interesting that these very local galaxies agree with our global value of H_0 . Furthermore, when V_{\odot} 's are corrected to the centroid of LG one observes a

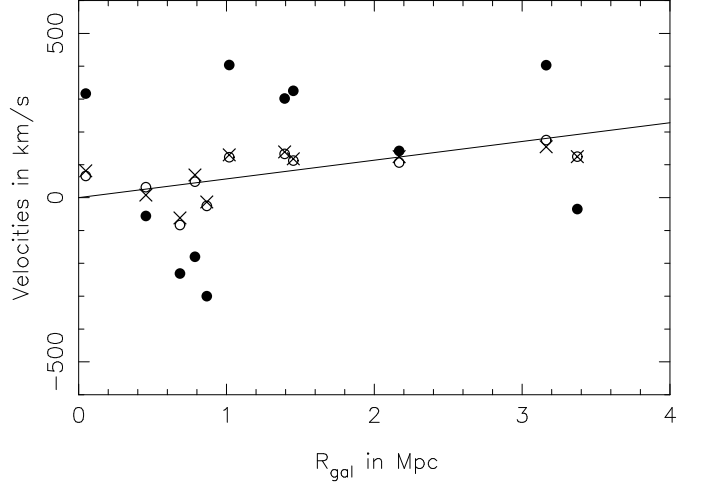


Fig. 3. The mean heliocentric velocities (filled circles) and velocities corrected to the centroid of the LG (according to Yahil et al. 1977: crosses; according to Richter et al. 1987: circles) for the nearest-by galaxies.

striking effect. In Fig. 3 one can see how the galaxies after the correction obey the Hubble law *all the way down to* $R_{\text{gal}} = 0$. The correction according to Yahil et al. (1977) are shown as crosses and according to Richter et al. (1987) as circles. It seems that it is a matter of taste which correction one prefers.

6. The virial mass of Virgo

6.1. Prediction from Model 1

Tully and Shaya (1984) estimated the virial mass of the Virgo cluster. Following the notation of Paper I the mass within $d = 0.105$, which corresponds to $\Theta = 6^\circ$ at the distance of Virgo, is:

$$\begin{aligned} M_{\text{virial}} &= 7.5 \times 10^{14} M_{\odot} R_{\text{Virgo}} / 16.8 \text{ Mpc} \\ &= 9.38 \times 10^{14} M_{\odot}, \end{aligned} \quad (17)$$

where the latter equality is based on the adopted distance $R_{\text{Virgo}} = 21 \text{ Mpc}$. With the cosmological parameters ($H_0 = 57 \text{ km s}^{-1} \text{ Mpc}^{-1}$ and $q_0 = 0.5$) and with our Model 1 we find using (Eq. 14 of Paper I)

$$M(d) = 14.76 \times q_0 h_0^2 \left[\frac{R_{\text{Virgo}}}{16.8 \text{ Mpc}} \right]^2 \times d^3 (1 + k' d^{-\alpha}), \quad (18)$$

where $h_0 = H_0 / 100 \text{ km s}^{-1} \text{ Mpc}^{-1}$, the mass within $d = 0.105$ in terms of M_{virial} :

$$M_{\text{pred}} = 1.62 \times M_{\text{virial}}. \quad (19)$$

The mass deduced agrees with the estimates 1.5-2.0 found by Paper I, where it was suspected that the virial mass estimation may come from a more concentrated area, which could explain the higher value obtained from the TB-solution.

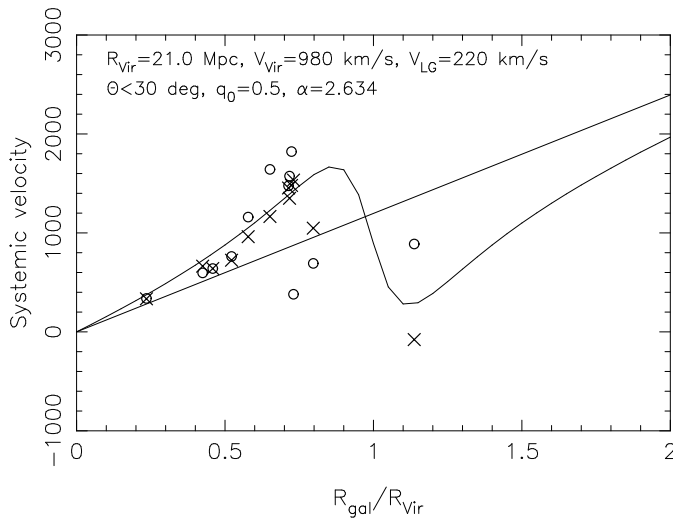


Fig. 4. The systemic velocity vs. distance for galaxies listed in Table 1 with $\alpha = 2.634$ (Model 3) predicting exactly one Virgo virial mass within a radius $d = 0.105$ from the Virgo. Circles refer to the observed velocities and crosses to the TB-predictions. The straight line is the Hubble law for $H_0 = 57 \text{ km s}^{-1} \text{ Mpc}^{-1}$ and the curve is the theoretical TB-pattern for $\Theta = 7^\circ$.

6.2. An alternative solution (Model 3)

We know all the parameters except α needed in Eq. 18. This led us make a test by looking for such an α which would bring about exactly one Virgo virial mass within the radius $d = 0.105$ from the Virgo center. We found $\alpha = 2.634$. The systemic velocity vs. distance diagram for this model 3 is given in Fig. 4. Again, NGC 4548 and NGC 4639 show anomalous behaviour. Comments made earlier are valid. There are three other galaxies showing a relatively large disagreement with the given TB-solution. NGC 4535 is close to Virgo at a small angular distance. Hence the arguments used for NGC 4639 are acceptable also here. Note that in Paper I this galaxy was classified as belonging to the region A, where galaxies are falling directly into Virgo. Furthermore, Federspiel et al. (1998) classifies this galaxy as a member of the subgroup B (these galaxies lie within 2.4° of M49). This clearly suggests a distortion in the velocity. NGC 4414 may belong to the Region B in Paper I. This could explain its low velocity. It is also rather close to the tangential point so that projection effects can be important. For NGC 4536 it is difficult to find any reasonable explanation. With these notes taken into account we conclude that model 3 cannot be excluded.

7. Conclusions

Studies of large-scale density enhancements in the Local Universe using spiral field galaxies – objects suitable for such a project – are discouraged by two factors. The observed distribution of spirals is rather irregular and the photometric distances based on Tully-Fisher relation are uncertain due to large scat-

ter. In the present work we avoided the latter problem up to a degree by using photometric distances from the extragalactic *PL*-relation. Such distances are far more accurate than Tully-Fisher distances.

It was quite satisfying to find out that the spherically symmetric TB-model predicts the observed velocity field well. As a matter of fact, in a recent study Hanski et al. (1999) implemented the TB-model to the mass determination of the Perseus-Pisces supercluster. Though the irregular behaviour of the luminous matter distribution is even more pronounced in Perseus-Pisces than in LSC the mass estimates were reasonable. These findings tend to indicate that the gravitating mass is more symmetrically distributed than the luminous matter indicates.

We found a solution (Model 1) predicting a Virgo cluster mass within $d_{21} = 0.105$ of $M_{\text{Virgo}} = 1.62 \times M_{\text{virial}}$ with M_{virial} given by Tully & Shaya (1984). This result is in agreement with Paper I, where the difference was suspected to mean that the virial mass is estimated from a more concentrated volume. Another plausible explanation is that Virgo is flattened. When presuming spherical symmetry under such condition more mass is required to induce the same effect on the velocities.

We were also able to find a solution predicting exactly one virial mass. Though this model does not agree with observations as well as Model 1 the fit is – considering the large uncertainties involved – acceptable.

We find these results significant in three ways. The intrinsic behaviour of the sample outside Virgo does not disagree with the global value of the Hubble constant $H_0 = 57 \text{ km s}^{-1} \text{ Mpc}^{-1}$. The TB-solutions agree with $R_{\text{Virgo}} = 21 \text{ Mpc}$, a value in excellent concordance with $R_{\text{Virgo}} = 20.7 \text{ Mpc}$ given by Federspiel et al. (1998). It is interesting also to be able to predict exactly one Virgo virial mass in the Einstein-deSitter universe, because in Paper I the mass predictions were larger than one and because $\Omega_0 = 1$ is strongly supported by theoretical considerations (both Inflation and Grand Unification require this value). Discussion on the cosmological constant Λ is postponed to a later phase of our research programme.

Having said all this one should be cautious. Results presented in this paper are based on frontside galaxies only. As can be seen from Fig. 4, in Paper I, predicted systemic velocities are more sensitive to the model parameters in the backside than in the front. In the next paper of this series we intend to find a few background galaxies with as reliable distance moduli as possible from other photometric distance estimators, in particular the Tully-Fisher relation with proper care taken of the selection effects.

Acknowledgements. This work has been partly supported by the Academy of Finland (project 45087: “Galaxy Streams and Structures in the nearby Universe” and project “Cosmology in the Local Universe”). We have made use of the Lyon-Meudon Extragalactic Database LEDA and the Extragalactic Cepheid Database. Finally we are grateful for the referee for constructive criticism and suggestions which have helped us to improve this paper.

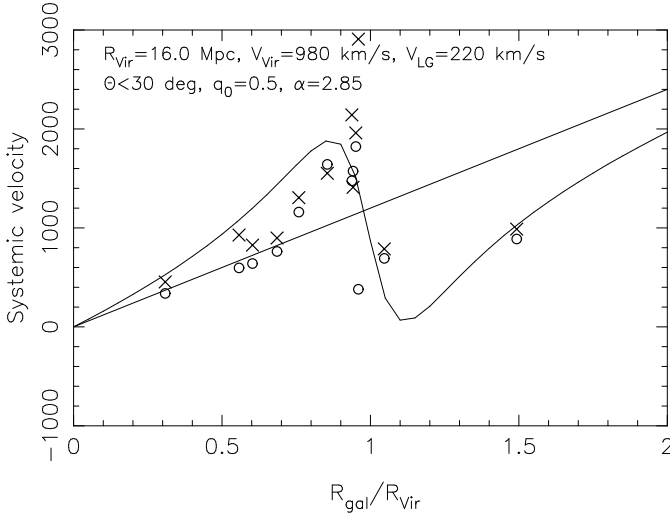


Fig. A.1. As Fig. 1 but now the distance to Virgo is $R_{\text{Virgo}} = 16$ Mpc.

Appendix A: Is $R_{\text{Virgo}} \approx 16$ Mpc?

In the present paper we fixed the distance to the centre of LSC by adopting a H_0 from external considerations and by fixing the cosmological velocity of the centre of LSC leading to $R_{\text{Virgo}} = 21$ Mpc. In Sect. 5.1 we noted that the galaxies outside the 30° cone measured from the centre of LSC do not allow us to exclude higher values of H_0 . Due to the fixed velocity these higher values, if really cosmological, necessarily lead to a shorter distance to the centre of LSC.

In this appendix we examine what happens to the TB pattern within the 30° cone where the TB model is relevant if we use $R_{\text{Virgo}} = 16$ Mpc. The result is shown in Fig. A.1. The infall pattern is still clearly present. The agreement between the observed points (circles) and the predicted points (crosses) is not as good as in Figs. 1 and 4. When Fig. A.1 is carefully compared with Fig. 1 one notes that in Fig. A.1 the observed systemic velocities are *systematically* smaller than the predicted ones. This is because for the shorter Virgo distance galaxies in front get closer to Virgo and thus the dynamical influence of Virgo should be larger. In Fig. 1 we observe no such systematic effect. It is thus possible to say that our sample is more favourable to a long distance scale than to a short scale.

We also examine the behaviour of the Hubble ratios $V_{\text{corr}}/R_{\text{gal}}$ as a function of V_{corr} (cf. Eq. 16). In Fig. A.2 the correction is based on $R_{\text{Virgo}} = 21$ Mpc and in Fig. A.3 on $R_{\text{Virgo}} = 16$ Mpc. The two values of H_0 used in Fig 2 are also given as straight horizontal lines. In both diagrams we observe increase in the Hubble ratios as V_{corr} increases starting at $V_{\text{corr}} \approx 600 \text{ km s}^{-1}$. In particular, for the shorter Virgo distance this effect is quite pronounced. Sandage and Tammann have on many occasion stressed that the value of the Hubble constant, H_0 , should not increase without any clear physical reason. In the absence of such the increase in H_0 is a warning signal that there is a bias present (e.g. the Malmquist bias). This is also our tentative interpretation for the increase in H_0 .

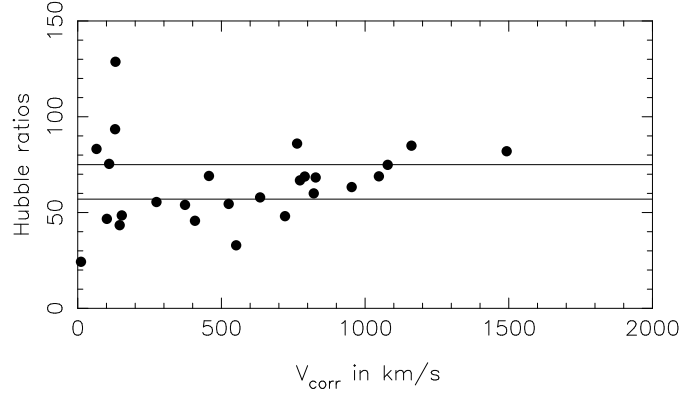


Fig. A.2. The Hubble ratios as a function of the corrected velocity for $R_{\text{Virgo}} = 21$ Mpc.

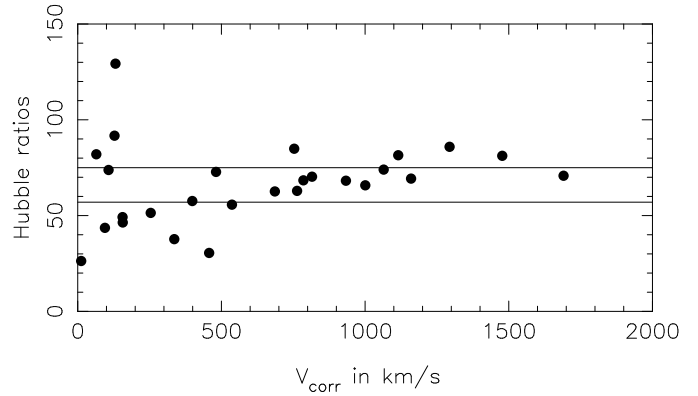


Fig. A.3. As Fig. A.2 but now $R_{\text{Virgo}} = 16$ Mpc.

One should also pay attention to the fact that in both cases the mean Hubble ratio is $\sim 55 \text{ km s}^{-1} \text{ Mpc}^{-1}$ for galaxies below $V_{\text{corr}} = 600 \text{ km s}^{-1}$.

However, part of the apparent increasing trend in H_0 could be an artefact of the velocity dispersion. If we overestimate the velocities galaxies have a tendency to move upwards and right. What is the nature of the suspected bias and its relation to the incompleteness bias of Lanoix et al. (1999c) as well as what is the influence of the velocity effect are amongst the topics we discuss in the next paper in this series.

References

- Bondi, H., 1947, MNRAS, 107, 410
- Ekholm, T., 1996 A&A 308, 7 (E96)
- Ekholm, T., Teerikorpi, P., 1994, A&A 284, 369 (ET94)
- Ekholm, T., Teerikorpi, P., Theureau, G. et al., 1999, A&A, 347, 99
- Federspiel, M., Tammann, G. A., Sandage, A., 1998, ApJ 495, 115
- Hanski, M., Theureau, G., Ekholm, T., Teerikorpi, P., 1999, submitted to A&A
- Lanoix, P., 1999, PhD Thesis, University of Lyon 1
- Lanoix, P., Paturel, G., Garnier, R., 1999a, MNRAS, in press
- Lanoix, P., Garnier, R., Paturel, G. et al., 1999b, Astron. Nach., 320, 21
- Lanoix, P., Paturel, G., Garnier, R., 1999c, ApJ 516, 188
- Olson, D. W., Silk, J., 1979, ApJ 233, 395

- Richter, O.-G., Tammann, G. A., Huchtmeier, W. K., 1987, A&A 171, 33
- Tammann, G. A., Sandage, A., 1985, ApJ 294, 81
- Teerikorpi, P., Bottinelli, L., Gouguenheim, L., Paturel, G., 1992, A&A 260, 17 (Paper I)
- Theureau, G., Hanski, M., Ekholm, T. et al., 1997, A&A 322, 730
- Tolman, R. C., 1934, Proc. Nat. Acad. Sci (Wash), 20, 169
- Tully, R. B., Shaya, E. J., 1984, ApJ 281, 31
- Yahil, A., Tammann, G. A., Sandage, A., 1977, ApJ 217, 903